Chemical Engineering Journal 162 (2010) 760–767

Contents lists available at ScienceDirect

Chemical Engineering Journal

journal homepage: www.elsevier.com/locate/cej

Mixing performance of unbalanced split and recombine micomixers with circular and rhombic sub-channels

Mubashshir Ahmad Ansari, Kwang-Yong Kim*

Department of Mechanical Engineering, Inha University, 253 Younghyun-dong, Nam-gu, Incheon 402-751, Republic of Korea

ARTICLE INFO

Article history:
Received 1 March 2010
Received in revised form 27 May 2010
Accepted 28 May 2010

Keywords:
Micromixer
Mixing index
Unbalanced split and recombine
Navier–Stokes equations
Pressure drop

ABSTRACT

Mixing performance has been evaluated for planar split and recombine micromixers with asymmetric sub-channels. The three-dimensional Navier–Stokes equations have been used to analyze fluid flow and mixing in a Reynolds number range from 1 to 80. The widths of the split channels are kept unequal to create unbalanced collisions of the fluid streams. Two shapes of the split channel have been considered; circular and rhombic. In the case of rhombic sub-channels, higher mixing is realized when width of the major sub-channel is either three or four times as wide as the minor sub-channel unlike the case of circular sub-channels. The results show the lowest mixing performance for the case of balanced collisions of fluid streams. The pressure-drop characteristic has been also analyzed at various Reynolds numbers.

1. Introduction

Mixing of fluids in channels of sub-millimeter dimensions is a fundamental operation required on microfluidic devices. The flow in such devices is laminar which makes it difficult to mix the fluids in a simple smooth microchannel. A wide variety of micromixers, operating on different mixing principles have been extensively reported by different researchers [1,2]. Micromixers can be broadly classified as active and passive micromixers. The active micromixers employ some external sources of energy to agitate the flow such as electric fields, magnetic fields, and acoustic waves [3–6]. Although active micromixers are effective in rapid mixing of the fluids, it is more difficult to fabricate, integrate and operate as compared to passive micromixers. The complex fabrication and integration of active micromixers with all operating devices is expensive and renders mass production difficult.

Passive micromixers are based on shape modification of the microchannels to produce a specific flow pattern which enhances mixing. The very basic design strategy is to make a series of bends to microchannels in different shapes, e.g., serpentine [7], zigzag [8], and curve [9], to create transverse flows to attain rapid mixing. Patterning on the wall floor with grooves to create chaotic flow has also been demonstrated to be utilized in mixing enhancement [10,11].

One of the important design categories of the passive micromixer belongs to split and recombine of microchannels [12–27] where the main channel is split into two or more streams and then the sub-channels recombine after certain distance in a repetitive fashion. The split sub-channels can be three-dimensional or planar. In three-dimensional split and recombine micromixers, the fluid streams are directed to create multiple interfaces. In such design, thus, the interface area increases gradually by directing the fluid streams in a specific pattern through the split channels and the length of diffusion for the molecules decreases which are favorable for effectively enhancing mixing [13–22]. However, the three-dimensional structure is difficult to fabricate and demands multiple steps in the microfabrication process as compared to planar split and recombine micromixers.

Planar split and recombine micromixers have been studied from simplest design with multiple streams [23–28]. Bessoth et al. [23] reported a design of planar split and recombine micromixer with a total of 32 streams, which showed efficient mixing. The major reason in attaining rapid mixing was the large number of streams. Jeon et al. [24] reported a micromixer with three sub-channels that explored the idea on recycle flow from two side channels joining the main central channel.

The simple split and recombine micromixers have been studied with some design modification to attain improved mixing. The design of the split and recombine micromixers with two channels has been modified by some researchers in order to attain rapid mixing [25–27]. Hong et al. [25] applied an innovative idea using modified Tesla structure for mixing in a wide range of flow rates. The design shows diffusive mixing at low flow rates and convective mixing at high flow rates. The main principle in mixing is Coanda effect which increases the transverse dispersion. The mixing efficiency was increased by providing constriction to the flow in the zone of split and recombine with the sub-channels of rhom-

* Corresponding author. Tel.: +82 32 872 3096; fax: +82 32 868 1716.
E-mail address: kykim@inha.ac.kr (K.-Y. Kim).

1385-8947/$ – see front matter © 2010 Elsevier B.V. All rights reserved.
doi:10.1016/j.cej.2010.05.068

bic shape [26,27]. The design of the split channels was modified to butterfly shaped with sharp folded channels for providing stirring action to mix the fluids with equal width of the two split channels [28]. These were few reported techniques to enhance mixing performance of the planar split and recombine micromixers.

In case of the split and recombine microchannel with two symmetric split sub-channels, it is difficult to mix the fluids at lower Reynolds numbers, where the mixing is mainly governed by molecular diffusion. In that case, the fluid streams will split and recombine without creating any perturbation to the interface of the fluid streams. The flow structure at a junction of split and recombine resembles to the flow in simple T-mixers where the two streams from the inlet channels come into contact at the T-junction. The design is effective in mixing of fluids only at higher Reynolds numbers [29,30]. At higher Reynolds numbers, collision of the fluid streams due to the effect of split and recombine improves mixing performance.

However, in the above mentioned planar split and recombine micromixers, the mixing is mainly due to constrictions to the flow [26,27]. The rhombic micromixer has constriction in the recombine zone and at the end of the micromixer. The idea of providing constriction to the flow is not novel as it can be applied to any design of microchannel in order to harness the reduced length of the diffusion for the fluid molecules for increasing mixing. Also, providing constriction to the flow will require higher pumping power due to higher pressure drop. However, in a planar micromixer with two splits without any constriction, the mixing will not be effective as it will create straight interface similar to T-mixers. The zone of recombination of the fluid streams can be the point of focus to convert simple recombination into collisions of the fluid streams to increase mixing. A basic concept of unbalanced collisions of fluid streams for enhancing mixing in planar split and recombine micromixers was proposed in a previous work [31] with numerical and experimental results for circular sub-channels. In this work, the remarkable effectiveness of the unbalanced collisions was verified by evaluating the mixing performance in comparison with the balanced collisions with symmetric sub-channels.

In the present work, the mixing performances of planar split and recombine micromixers with rhombic and circular sub-channels are evaluated numerically when the design of unbalanced collisions [31] is introduced. The analyses of the flow and mixing have been performed by solving three-dimensional Navier–Stokes equations in a range of Reynolds number from 1 to 80. The main channel of the micromixers is split into two subchannels (rhombic or circular shape) of unequal widths in a repeating manner. The micromixer has been analyzed by fixing the flow area in the sub-channels for different levels of unbalance in the collisions controlled by varying the width ratio of the split subchannels.

2. Micromixer model and numerical analysis

Fig. 1 shows the schematic models of the micromixer with the main channel splitting into two sub-channels of unequal widths for circular (Fig. 1(a)) and rhombic (Fig. 1(b)) shapes. The micromixers have total four units of split and recombination. The sub-channels with wider width has been named as major sub-channels while the other as minor sub-channels. The main idea of asymmetric sub-channels is to create unbalance collisions due to the difference in the inertia of the fluid streams from two sub-channels to enhance mixing.

The various dimensions of the micromixer are $w = 300\,\mu m$, Lo = 500 μm, Le = 2.95 m, and d_o = 900 μm. The pitch, Pi (=1.2 mm), is fixed and the same in both cases (circular and rhombic sub-channels). The widths of the sub-channels are varied with fixed total width which equals to the width of the main channel ($w_1 + w_2 = w = 300\,\mu m$) in order to maintain constant area of flow. The widths of the main channel, major and minor sub-channels are denoted by w, w_1 and w_2, respectively. In varying the widths of the sub-channels, the outer wall is shifted keeping the inner wall fixed for both circular and rhombic shapes. The height of the micromixer model has been kept constant at 200 μm for both circular and rhombic shapes.

The steady, incompressible flows in the micromixers are analyzed by solving three-dimensional continuity and Navier–Stokes equations:

$$\nabla \cdot \vec{V} = 0 \tag{1}$$

$$\rho(\vec{V} \cdot \nabla)\vec{V} = \nabla p + \mu \nabla^2 \vec{V} \tag{2}$$

Computational domain has been discretized by structured grids. The mesh density was kept high near the zone of split and collision of the fluid streams. The details of the numerical methods including numerical schemes and discretization methods can be found in the previous paper [32]. Ethanol and water have been selected as the working fluids for mixing analysis. The two inlets have been assigned with 100% water and 100% ethanol, respectively, which come into contact at the T-junction and the pass through a series of the split and recombine mixing segments. The inlets and outlet have been assigned uniform velocity profile and zero static pressure as boundary conditions. The Walls have been assigned no slip boundary condition. The properties of the water and ethanol are measured at 20 °C. The diffusivity of water and ethanol is commonly taken as $1.2 \times 10^{-9}\ m^2\ s^{-1}$. The densities of water and ethanol are 9.97×10^2 and $7.89 \times 10^2\ kg/m^3$, respectively.

Along with investigating the mixing and flow field in the micromixer, it is critical to quantify mixing in order to compare the mixing performance of different designs. The mixing performance of the micromixer has been measured by calculating the mixing index from the variance of the mass fraction on planes perpendicular to x-axis defined as follows:

$$\sigma^2 = \frac{1}{N}\sum (c_i - \bar{c}_m)^2 \tag{3}$$

$$M = 1 - \sqrt{\frac{\sigma^2}{\sigma^2_{max}}} \tag{4}$$

where σ^2 is the variance, σ^2_{max} is maximum variance of the fluid mixture, c_i is the mass fraction at ith sampling point on the plane. $\bar{c}_m$ is the optimal mixing mass fraction and M is the mixing index. N represents the number of the sampling points for the concentration on the plane. M_o denotes the value of the mixing index at 5.5 mm downstream of the end of the last sub-channels.

3. Results and discussion

The mixing performance and fluid flow in the design of the micromixers based on unbalanced spits and collisions of the fluid streams [31] has been analyzed numerically. Fig. 2 shows the samples of structured grid systems for circular and rhombic sub-channels, respectively. The mesh density is adjusted so that it becomes higher near the regions where the split and cross-collision of fluid streams take place. Fig. 3 shows the results of the grid independency test with five different grid systems wherein the number of nodes ranges from 320×10^3 to 2250×10^3 for circular sub-channels with $w_1/w_2 = 2.0$. From the results of this test, the grid system with 1560×10^3 nodes has been selected as the optimum grid system on which further analyses are performed.

Fig. 4 shows the contour-plot of the velocity field on the xy-plane for circular sub-channels with $w_1/w_2 = 2.0$ at Re = 60. Throughout the micromixer that is comprised of four segments, the velocity in

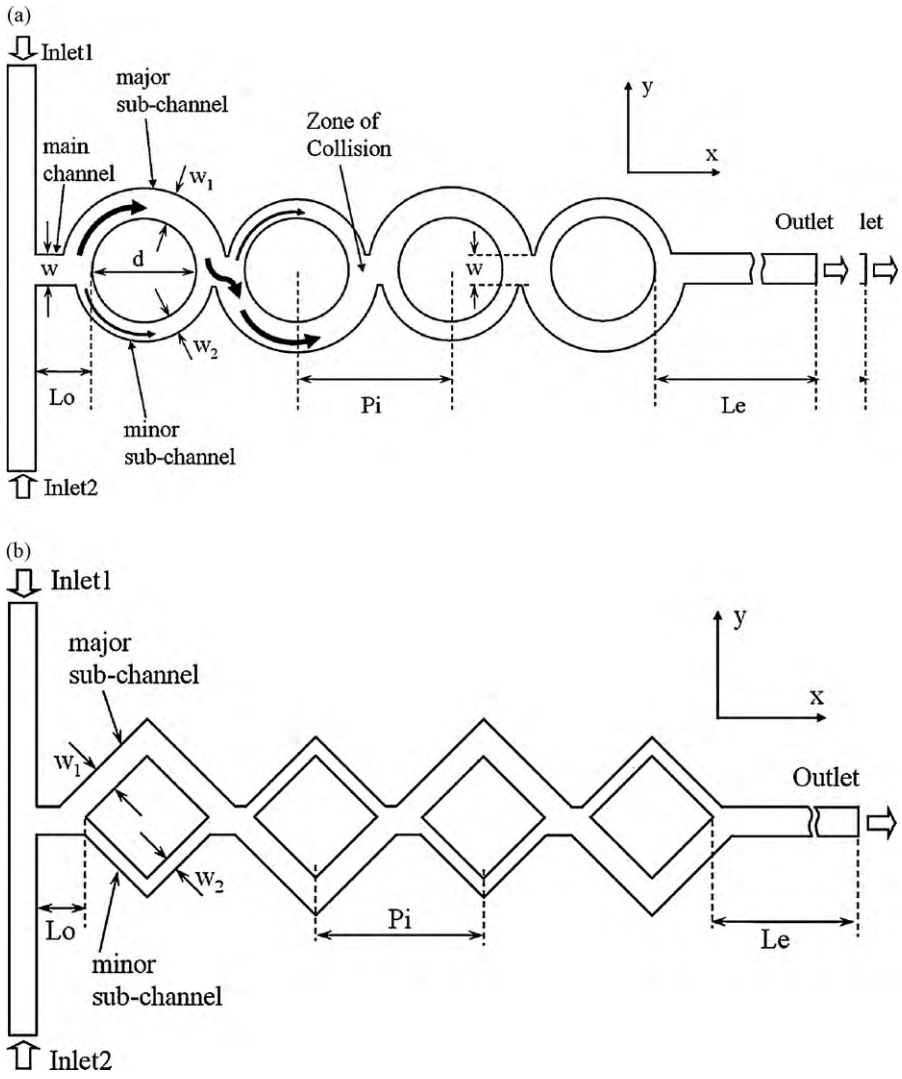

Fig. 1. Schematic diagrams of unbalanced splits and cross-collisions: (a) circular sub-channels [31]; (b) rhombic sub-channels.

the major sub-channel is higher than that in the minor sub-channel. The difference in the velocity between the major and minor sub-channels is the key feature that creates an unbalanced collision of the fluid streams.

Fig. 5(a) and (b) respectively show the mass-fraction distributions of ethanol for circular and rhombic sub-channels on the *xy*-plane in the cross-section that is midway along the channel-height of the micromixer. The effect of the ratio of widths on mixing is shown for three values of w_1/w_2, namely, 1.0, and 2.0, at Re = 60. $w_1/w_2 = 1.0$ corresponds to the case of balanced collision of the fluid streams. The flows from the two sub-channels undergo splitting and collision in the sub-channels. In the case of equal widths, the interface of the two fluids almost coincides with the plane of symmetry of the micromixer. Thus, the area of the interface is restricted to only the splitting-collision zones. On the other hand, the contour-plots for $w_1/w_2 = 2.0$ correspond to unbalanced collisions of fluid streams, as shown in Fig. 5(a) and (b). In this case, the interface of the two fluids is not restricted to the small regions of splitting and collision, but extends to the full length of the sub-channels of the micromixer. This is attributed to unbalanced cross-collisions. Unlike the case of balanced collision, the interface of the two fluids is clearly seen in the circular or rhombic sub-channels; the increased area of the interface enhances the mixing.

Fig. 6 shows the effect of w_1/w_2 on the mixing index for rhombic sub-channels from Re = 1 to Re = 80. The mixing index as a function of w_1/w_2 ratio for circular sub-channels has been reported in the previous paper [31] which shows gradual increase in the mixing index to reach its maximum at $w_1/w_2 = 2.0$. Till $w_1/w_2 = 2.0$, the trend of variation of the mixing index with w_1/w_2 is almost the same as for circular sub-channels [31] at all Reynolds numbers. However, unlike the case of circular sub-channels, the highest value of the mixing index is not realized at $w_1/w_2 = 2.0$. Rather, the mixing index continues to increase gradually, even beyond $w_1/w_2 = 2.0$ and till $w_1/w_2 = 3.0$. Beyond $w_1/w_2 = 3.0$, the mixing index is almost constant and shows very slight variation till $w_1/w_2 = 4.0$. Higher mixing performance is shown at higher Reynolds numbers for both types of sub-channel. However, even at low Reynolds numbers, the mixing index increases with w_1/w_2.

Fig. 7 shows the comparison of the mixing index for the circular and rhombic sub-channels at various Reynolds numbers with $w_1/w_2 = 2.0$ and $w_1/w_2 = 3.0$, respectively. The main objective is to analyze and select the design of the micromixer so that the mixing performance is maximized. At low Reynolds numbers, i.e., 1, 10, and 20, where the mixing index decreases with the Reynolds number, the mixing index is not affected by any design configuration, and shows the same mixing performance for both circular and rhombic sub-channels. However, at higher Reynolds numbers,

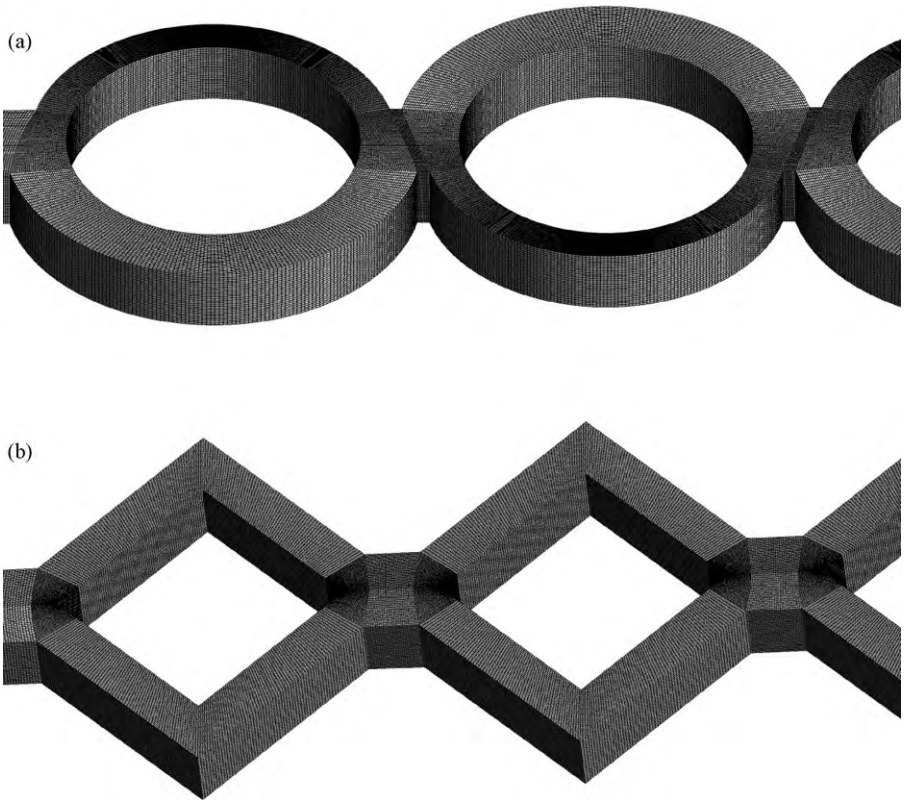

Fig. 2. Examples of grid system: (a) circular sub-channels, $w_1/w_2 = 1.7$; (b) rhombic sub-channels, $w_1/w_2 = 1.0$.

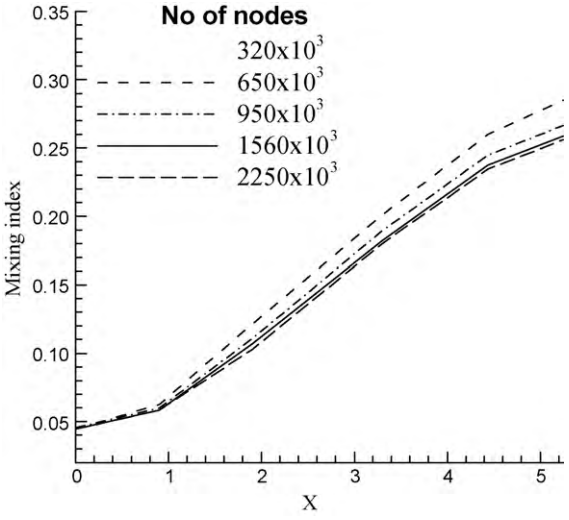

Fig. 3. Test of grid independency ($w_1/w_2 = 2.0$).

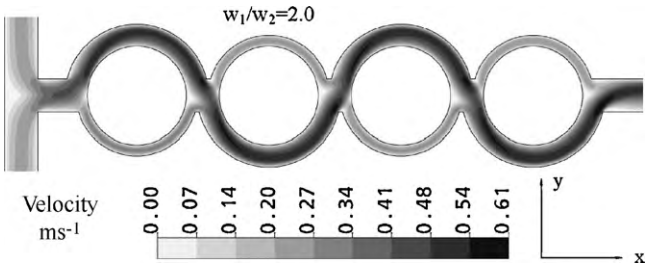

Fig. 4. Velocity contours in circular sub-channels on the *xy*-plane in the cross-section that is midway along the channel-height ($w_1/w_2 = 2.0$ and Re = 60).

i.e., 40, 60, and 80, the mixing varies with various design configurations. The circular sub-channels with $w_1/w_2 = 2.0$ show the highest mixing performance among all the cases analyzed in the present study. The micromixer with rhombic sub-channels generally shows lower mixing performance as compared to the one with circular sub-channels. Thus, the micromixer with circular sub-channels is the proposed design that can be effectively used to mix the fluids. The possible reason for higher mixing performance by circular sub-channels is the presence dean vortices in the entire length of the split sub-channels due to uniform curve. Whereas, in rhombic sub-channel, there is only one sharp bend and the rest part is straight.

For $w_1/w_2 = 2.0$, Fig. 8 shows the mass-fraction distribution of ethanol on the *yz*-plane that is perpendicular to the direction of the main flow in the middle of the second set of circular sub-channels at six different Reynolds numbers. At Re = 1 and Re = 10, the interface between the fluids is nearly vertical in the major sub-channel, while only single fluid is present in the minor sub-channel. This is because at these low Reynolds numbers, the inertial force is relatively very weak and unable to create transverse flows in the sub-channel. Hence, mixing relies mainly on diffusion, as shown in Fig. 9. However, as the Reynolds number increases, the interface between the fluids bends, which increases the area of the interface over which mixing takes place by the diffusion of the fluids. Also, the proportion of the second fluid in minor sub-channels increases. The bending of the interface is symmetrical to the horizontal plane near the mid-point of the channel-height. This is likely due to the symmetrical transverse flow structures that are developed in the channel, as can be seen in Fig. 9.

Fig. 9 shows the velocity-vector plots for the same operating condition presented in Fig. 8. At Reynolds numbers larger than 10, two vortices are clearly visible in the major sub-channel while the vortical flows are hardly found in the minor sub-channel at lower Reynolds numbers. Although these Dean vortices are present in the

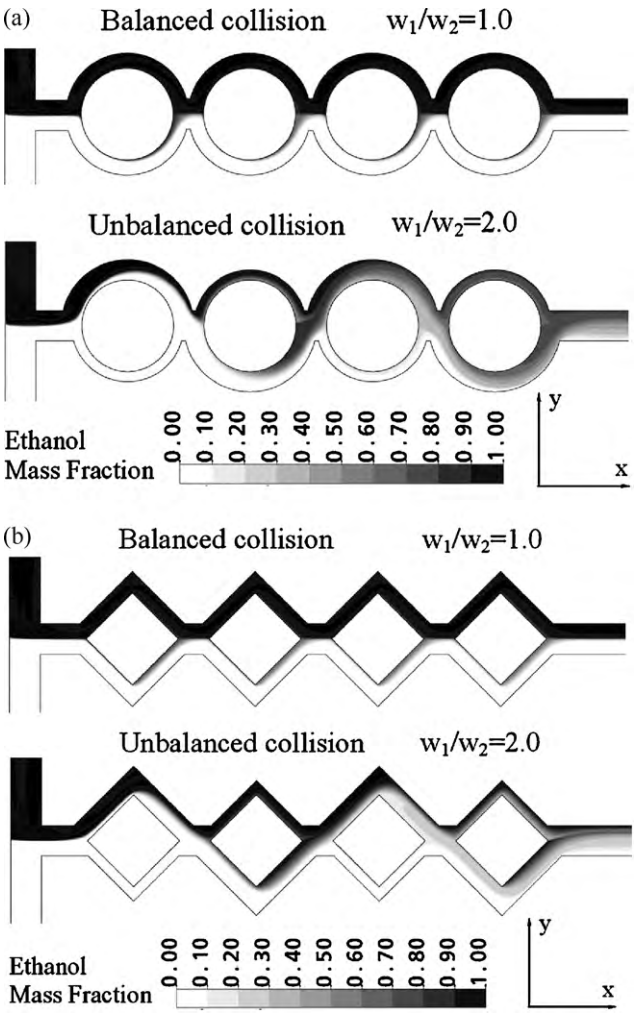

Fig. 5. Distributions of the mass-fraction of ethanol at Re = 60 on the *xy*-plane in the cross-section that is midway along the channel-height: (a) circular sub-channels and (b) rhombic sub-channels for balanced and unbalanced collisions of fluid streams.

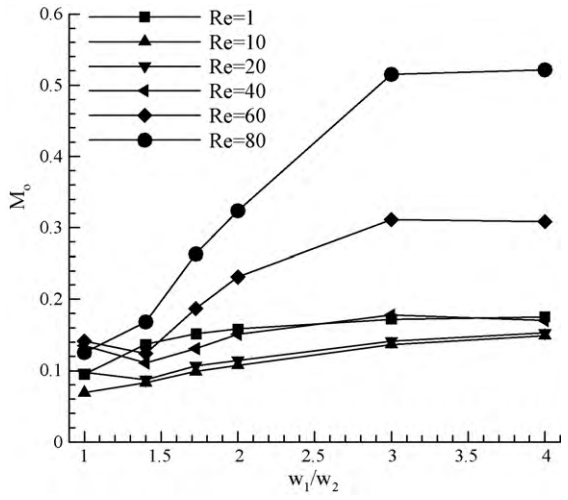

Fig. 6. The mixing index at the end of the micromixer, M_o, vs. the ratio of w_1/w_2 for rhombic sub-channels at various Reynolds numbers.

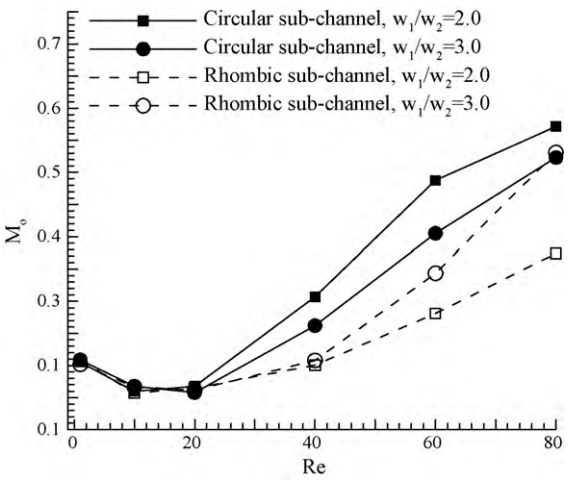

Fig. 7. Variations of the mixing index with Re for various combinations of the channel split.

major sub-channel at Re = 10, they are not able to significantly influence the interface of the fluid as shown in Fig. 8, and are therefore less effective for mixing. However, at Re = 20, the interface between the fluids is significantly perturbed or stretched, a phenomenon that gradually becomes more pronounced with the Reynolds number.

The mechanism of mixing in unbalanced split and recombine micromixer can be understood by analyzing the above results. Mixing in this micromixer is mainly contributed by three different processes; diffusion, dean vortices and unbalanced split and collisions of fluid streams. Fig. 7 indicates that at Reynolds numbers less than 20 the main mechanism of mixing is diffusive mixing over the interface of the fluid streams as the different designs of micromixer have no influence on the mixing performance. Among the three

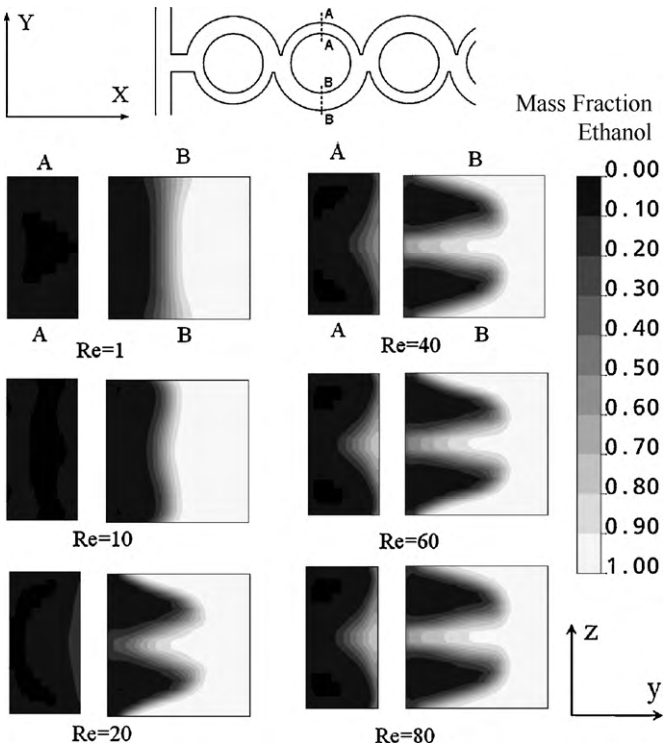

Fig. 8. Mass-fraction distributions for circular sub-channels at different Reynolds numbers for $w_1/w_2 = 2.0$.

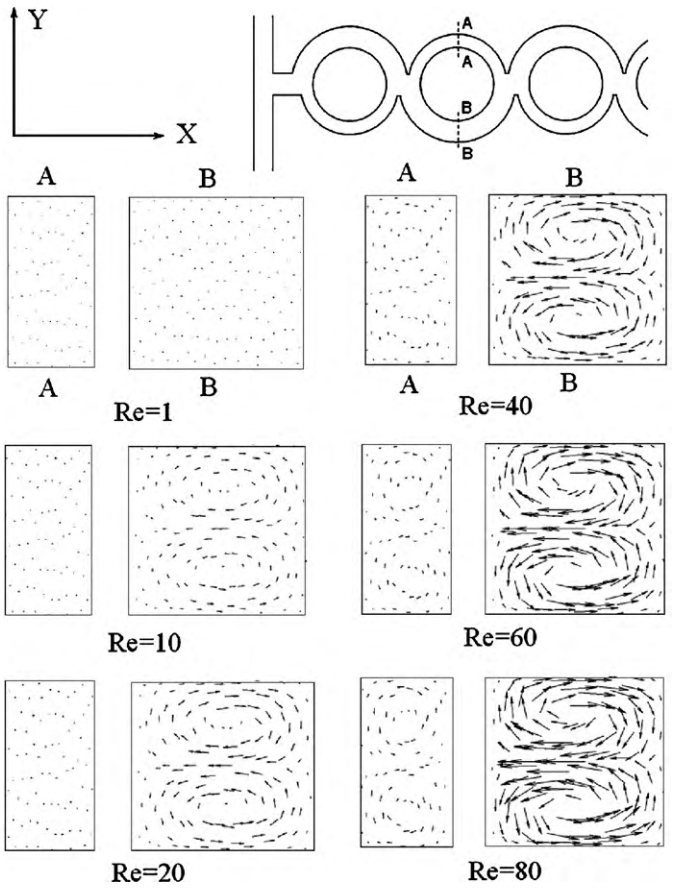

Fig. 9. Vector plots on the *yz*-plane for circular sub-channels at different Reynolds numbers for $w_1/w_2 = 2.0$.

Reynolds numbers in the range of diffusive mixing, higher mixing at Re = 1 is apprehended due to longer residence time of the fluid streams. Unbalanced collision of fluid streams is contributing to mixing by controlling the position of the interface (increasing interface area by shifting to major sub-channel). Dean vortices formed in the sub-channels (Fig. 9) starts to increase the interface area of the fluid streams at Re = 20 as shown in Fig. 8. As the overlapping mixing curve from Reynolds number 1 to 20 starts to show variation beyond Re = 40 as shown in Fig. 7, the dean vortices and unbalanced collisions of the fluid streams start to contribute to mixing in this range of Reynolds number. The effect of the different designs of the micromixer on mixing becomes more obvious at higher Reynolds number.

For the cases of circular and rhombic sub-channels, Fig. 10 shows the contour-plots of the mass-fraction of ethanol on the *xy*-plane in the cross-section that is midway along the channel-height in the case where all the major sub-channels are located only on one side of the *x*-axis. The fluids from Inlet 1 and Inlet 2, respectively, flow through the micromixer only along their own respective sides and do not cross each other. However, the design is still showing better mixing performance as compared to balanced collisions of the fluid streams.

Fig. 11(a) and (b) show the effect of the position of the major sub-channels along the *x*-axis on the mixing index for circular and rhombic sub-channels, respectively. The proposed design, wherein the major sub-channels are interchanged with the minor sub-channels, is compared with the case where the major sub-channels are located only on one side of the *x*-axis. The mixing index, M_o, has been calculated at 5.5 mm downstream of the end of the last sub-channels with $w_1/w_2 = 2.0$ for both circular and rhombic

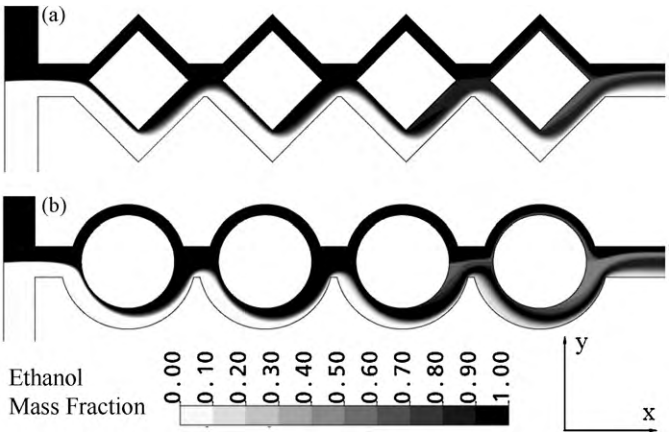

Fig. 10. Distributions, at Re = 60, of the mass-fraction of ethanol, on the *yz*-plane in the cross-section that is midway along the channel-height, for major sub-channels on the same side of the *x*-axis: (a) rhombic sub-channels; (b) circular sub-channels.

sub-channels. In the case where the positions of the major sub-channels are shifted, both the circular and rhombic sub-channels show obviously greater mixing performance at all Reynolds numbers. However, in the case of circular sub-channels, the effect is more prominent.

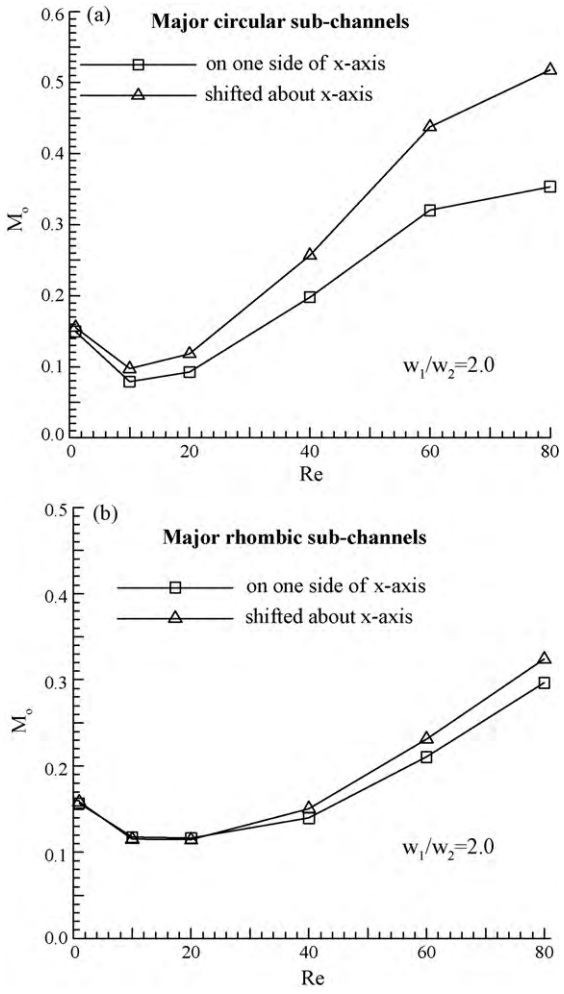

Fig. 11. Effects of the positions of the major sub-channels on the mixing index at the end of the micromixer at different Reynolds numbers: (a) circular sub-channels; (b) rhombic sub-channels.

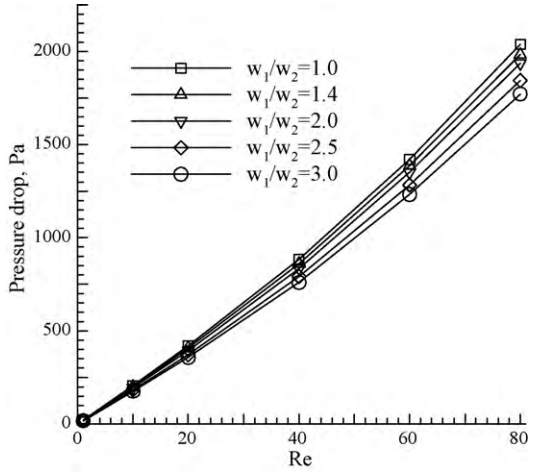

Fig. 12. The pressure-drop vs. Re for circular sub-channels at various ratios of w_1/w_2.

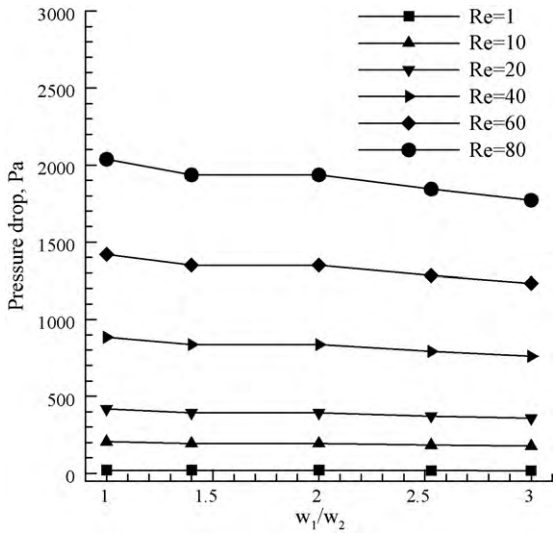

Fig. 13. The pressure-drop as a function of the ratio of w_1/w_2 for rhombic sub-channels.

Fig. 12 shows the characteristics of the pressure-drop as a function of the Reynolds number at various values of w_1/w_2 for circular sub-channels. The pressure-drop has been calculated for a fixed length of the micromixer. The pressure-drop increases with the Reynolds number for both circular and rhombic sub-channels. The effect of w_1/w_2 becomes larger at higher Reynolds numbers. Fig. 13 shows the effect of w_1/w_2 on the pressure-drop for rhombic sub-channels at various Reynolds numbers. For a given Reynolds number, the pressure-drop decreases with w_1/w_2. The sub-channel with equal widths (balanced collision) shows the greatest pressure-drop at all Reynolds numbers, which is disadvantageous as far as pumping power is concerned. Thus, the design with unbalanced collisions yields better performance for the pressure-drop as well.

4. Conclusion

Numerical study has been conducted to investigate mixing and the flow field on a number of planar split and recombine micromixer designs to find the best condition that yields high mixing performance. Analysis has been carried out on two types of unbalanced splits and cross collisions, one with circular sub-channels and another with rhombic sub-channels, for a wide range of the Reynolds number, i.e., from 1 to 80. In the case of rhombic sub-channels, the highest performance is realized at $w_1/w_2 = 3.0$ or 4.0 depending the Reynolds number unlike the case of circular sub-channels which shows the highest mixing performance at $w_1/w_2 = 2.0$. The result shows the lowest mixing performance for sub-channels of equal width (balanced collision) in both circular and rhombic sub-channels at all Reynolds numbers. The overall comparison of the mixing index across various geometries of the micromixer shows high mixing performance for circular sub-channels with $w_1/w_2 = 2.0$. Flow-field analysis has been undertaken to understand the mixing behavior that is exhibited by different shapes of the micromixer. The pressure-drop is lower for unbalanced collision as compared to balance collision, which is advantageous as far as pumping power is concerned.

Acknowledgments

This work was supported by the National Research Foundation of Korea (NRF) grant No. 2009-0083510 funded by the Korean government (MEST) through Multi-phenomena CFD Engineering Research Center.

References

[1] N.T. Nguyen, Z.G. Wu, Micromixers—a review, J. Micromech. Microeng. 15 (2005) R1–R16.
[2] V. Hessel, H. Lowe, F. Schonfeld, Micromixers—a review on passive and active mixing principles, Chem. Eng. Sci. 60 (2005) 2479–2501.
[3] K. Sritharan, C.J. Strobl, M.F. Schneider, A. Wixforth, Z. Guttenberg, Acoustic mixing at low Reynold's numbers, Appl. Phys. Lett. 88 (2006) 054102.
[4] M.H. Oddy, J.G. Santiago, J.C. Mikkelsen, Electrokinetic instability micromixing, Anal. Chem. 73 (2001) 5822–5832.
[5] L.H. Lu, K.S. Ryu, C. Liu, A magnetic microstirrer and array for microfluidic mixing, J. Microelectromech. Syst. 11 (5) (2002) 462–469.
[6] X.Z. Niu, L.Y. Liu, W.J. Wen, P. Sheng, Active microfluidic mixer chip, Appl. Phys. Lett. 88 (2006).
[7] R.H. Liu, M.A. Stremler, K.V. Sharp, M.G. Olsen, J.G. Santiago, R.J. Adrian, H. Aref, D.J. Beebe, Passive mixing in a three-dimensional serpentine microchannel, J. Microelectromech. Syst. 9 (2) (2000) 190–197.
[8] V. Mengeaud, J. Josserand, H.H. Girault, Mixing processes in a zigzag microchannel: finite element simulations and optical study, Anal. Chem. 74 (2002) 4279–4286.
[9] F. Schonfeld, S. Hardt, Simulation of helical flows in microchannels, AIChE J. 50 (2004) 771–778.
[10] A.D. Stroock, S.K.W. Dertinger, A. Ajdari, I. Mezic, H.A. Stone, G.M. Whitesides, Chaotic mixer for microchannels, Science 295 (2002) 647–651.
[11] T.J. Johnson, D. Ross, L.E. Locascio, Rapid microfluidic mixing, Anal. Chem. 74 (2002) 45–51.
[12] N. Schwesinger, T. Frank, H. Wurmus, A modular microfluid system with an integrated micromixer, J. Micromech. Microeng. 6 (1996) 99–102.
[13] F. Schonfeld, V. Hessel, C. Hoffmann, An optimised split-and-recombine micromixer with uniform 'chaotic' mixing, Lab Chip 4 (2004) 65–69.
[14] D.S. Kim, S.H. Lee, T.H. Kwon, C.H. Ahn, A serpentine laminating micromixer combining splitting/recombination and advection, Lab Chip 5 (2005) 739–747.
[15] H.M. Xia, S.Y.M. Wan, C. Shu, Y.T. Chew, Chaotic micromixers using two-layer crossing channels to exhibit fast mixing at low Reynolds numbers, Lab Chip 5 (2005) 748–755.
[16] H. Chen, J.C. Meiners, Topologic mixing on a microfluidic chip, Appl. Phys. Lett. 84 (2004) 2193–2195.
[17] S.W. Lee, D.S. Kim, S.S. Lee, T.H. Kwon, A split and recombination micromixer fabricated in a PDMS three-dimensional structure, J. Micromech. Microeng. 16 (2006) 1067–1072.
[18] S.W. Lee, S.S. Lee, Rotation effect in split and recombination micromixing, Sens. Actuators B 129 (2008) 364–371.
[19] J.M. Park, D.S. Kim, T.G. Kang, T.H. Kwon, Improved serpentine laminating micromixer with enhanced local advection, Microfluid. Nanofluid. 4 (2008) 513–523.
[20] A.P. Sudarsan, V.M. Ugaz, Multivortex micromixing, Proc. Natl. Acad. Sci. U.S.A. 103 (2006) 7228–7233.
[21] L.L. Wang, J.T. Yang, An overlapping crisscross micromixer using chaotic mixing principles, J. Micromech. Microeng. 16 (2006) 2684–2691.
[22] C. Simonnet, A. Groisman, Chaotic mixing in a steady flow in a microchannel, Phys. Rev. Lett. 94 (2005).
[23] F.G. Bessoth, A.J. deMello, A. Manz, Microstructure for efficient continuous flow mixing, Anal. Commun. 36 (1999) 213–215.
[24] M.K. Jeon, J.H. Kim, J. Noh, S.H. Kim, H.G. Park, S.I. Woo, Design and characterization of a passive recycle micromixer, J. Micromech. Microeng. 15 (2005) 346–350.
[25] C.C. Hong, J.W. Choi, C.H. Ahn, A novel in-plane passive microfluidic mixer with modified Tesla structures, Lab Chip 4 (2004) 109–113.

[26] C.K. Chung, T.R. Shih, A rhombic micromixer with asymmetrical flow for enhancing mixing, J. Micromech. Microeng. 17 (2007) 2495–2504.
[27] C.K. Chung, T.R. Shih, Effect of geometry on fluid mixing of the rhombic micromixers, Microfluid. Nanofluid. 4 (2008) 419–425.
[28] Z. Lu, J. McMahon, H. Mohamed, D. Barnard, T.R. Shaikh, C.A. Mannella, T. Wagenknecht, T.M. Lu, Passive microfluidic device for submillisecond mixing, Sens. Actuators B 144 (1) (2009) 301–309.
[29] N. Kockmann, T. Kiefer, M. Engler, P. Woias, Convective mixing and chemical reactions in microchannels with high flow rates, Sens. Actuators B 117 (2006) 495–508.
[30] M. Engler, N. Kockmann, T. Kiefer, P. Woias, Numerical and experimental investigations on liquid mixing in static micromixers, Chem. Eng. J. 101 (2004) 315–322.
[31] M.A. Ansari, K.Y. Kim, K. Anwar, S.M. Kim, A novel passive micromixer based on unbalanced splits and collisions of fluid streams, J. Micromech. Microeng. 20 (2010) 055007.
[32] M.A. Ansari, K.Y. Kim, A numerical study of mixing in a microchannel with circular mixing chambers, AIChE J. 55 (9) (2009) 2217–2225.